Ferroelectric properties of triangular charge-frustrated $LuFe_2O_4$

2008 J. Phys.: Condens. Matter 20 434218

(http://iopscience.iop.org/0953-8984/20/43/434218)

J. Phys.: Condens. Matter **20** (2008) 434218 (6pp) doi:10.1088/0953-8984/20/43/434218

Ferroelectric properties of triangular charge-frustrated $LuFe_2O_4$

Naoshi Ikeda

Department of Physics, Okayama University, Tsushima-naka, Okayama 700-8530, Japan

E-mail: ikedan@science.okayama-u.ac.jp

Received 21 April 2008, in final form 14 July 2008
Published 9 October 2008
Online at stacks.iop.org/JPhysCM/20/434218

Abstract

Magnetic and dielectric correlation in triangular mixed valence iron oxide RFe_2O_4 is discussed. The frustrated interaction for antiferromagnetic spins as well as charges realizes the auto-organized superlattice cell of iron ions. The characteristic charge and spin superlattice cell drives the magnetoelectric cross-correlation. The charge supercell detected with a resonant x-ray scattering measurement has an electric polarization that forms a class of new ferroelectrics.

1. Introduction

3D electrons in transition metal ions possess degrees of freedom in spin charge and orbitals. Their cross-correlation brings a wide variety of phenomena that have been of interest in the physics and chemistry of solids for a long time. Among the unique properties of transition metal compounds, the correlation between magnetism and ferroelectricity is an old but still current topic [1–3]. The mechanism of ferroelectricity has been understood as the cooperative appearance of electric dipoles that arise from the displacement of anion and cation pairs in crystals. Magnetism is the cooperative phenomena of spins on the transition metal ion. Their correlated interaction is the so-called magnetoelectric interaction phenomena. The charge and spin frustration in RFe_2O_4 is considered to have such a coupling between spin and charge coherence. As the detailed mechanism is not fully understood, the electric polarization coherence is considered to connect to the development of the spin coherence. Current information on the correlated structure for the spin and the charge is described here.

The RFe_2O_4 system (R = Y, In, Sc and Dy to Lu) has a hexagonal structure with the space group of $R\bar{3}m$ (166) [4]. The crystal structure consists of alternate stacking of triangular lattices along the c axis, as shown in figure 1. The double iron triangular layer (W layer) is separated by a single rare earth triangular layer (T layer) in the structure. In the W layer, the iron has fivefold oxygen coordination with a triangular bi-pyramid. The rare earth ion is positioned in a distorted oxygen octahedron. The valence state of the iron ion is mixed as a result of the coexistence of Fe^{3+} and Fe^{2+}. With the triangular lattice structure, it is a frustrated system with respect to the nearest-neighbor interactions between Fe ions. This fact is reflected in several interesting magnetic and electric properties of this system.

2. Magnetic properties of RFe_2O_4

The layered structure is responsible for the two-dimensional character of this system. The spin or charge coupling of irons within an a–b plane is stronger than that along the c axis, which brings about the anisotropic ordering process of the spin and charges. Such electronic ordering of irons occurs in the Fe W layer. Furthermore, the oxygen deficiency δ in the expression of $RFe_2O_{4-\delta}$ is a sensitive parameter correlated with the electronic and magnetic properties of this system. Generally, the ordering of the spin or charges within the a–b plane (so-called two-dimensional ordering) becomes more dominant in a system having larger δ (having a large amount of oxygen deficiency) or smaller rare earth ions.

Generally, RFe_2O_4 shows a magnetic transition at about 240 K [4]. The spontaneous magnetic moment evaluated from the saturated magnetization measurement is approximately $1.4\mu_B$/f.u., which indicates the spin arrangement is not ferromagnetic. The magnetization has strong uniaxial anisotropy with the easy axis along the c direction [5]. This fact is interpreted as the ferrimagnetic ordering of Fe^{2+} and Fe^{3+}. The strong magnetic anisotropy originates from the fivefold oxygen coordination of Fe ions.

From the neutron diffraction study [6] of the less-stoichiometric YFe_2O_4, the Bragg line indexed as $(1/3\ 1/3\ l)$, where l is a continuous value, was found. The presence of the

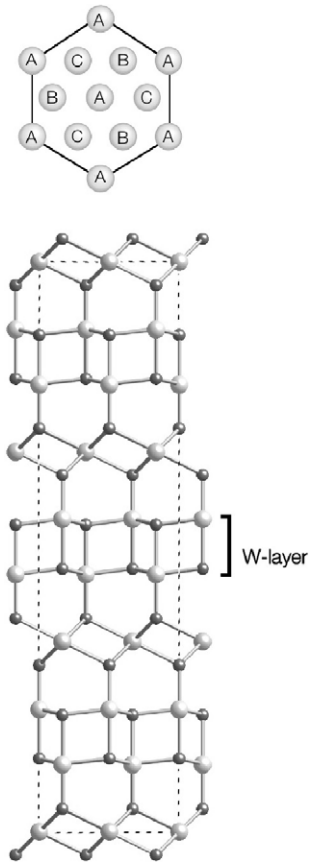

Figure 1. Crystal structure of RFe_2O_4 as a stacking of triangular lattices. Although the space group is rhombohedral, a hexagonal cell is drawn in the dotted area. The upper hexagon indicates the relative atomic position A, B and C in the triangular lattice.

Bragg line indicates that the developed spin correlation exists only within the *a*–*b* plane. The two-dimensional magnetic cell is elongated along the [1 1 0] direction and is three times larger than the chemical cell. The spin correlation length along the *c* axis is smaller than that in the *a*–*b* plane.

In some cases, the less-oxygen-deficient sample two-dimensional spin ordering becomes a three-dimensional one in the low-temperature region, as in examples reported for stoichiometric YFe_2O_4 [7] and $ErFe_2O_4$ [8]. As for the charge ordering of $LuFe_2O_4$, which will be discussed later, a diffraction study [9] has revealed that the three-dimensional ordering remains up to 330 K, that is, higher than the spin-ordering temperature of 240 K. Above 330 K, the charge ordering becomes two-dimensional.

Mössbauer spectroscopy studies under a magnetic field [10] yielded information about the spin arrangement in the Fe W layer. The analysis of the absorption spectra in the function of the magnetic field indicated that both Fe^{2+} and Fe^{3+} ions are classified into three different groups according to their electric and magnetic environments. One-third of the Fe^{3+} spins were parallel to the magnetization, while the remaining 2/3 were in the opposite direction. In a comparison of these findings with saturated magnetization, it was concluded that $YbFe_2O_4$ had ferrimagnetic ordering, where 2/3 of Fe^{2+} spins were parallel to the magnetization and

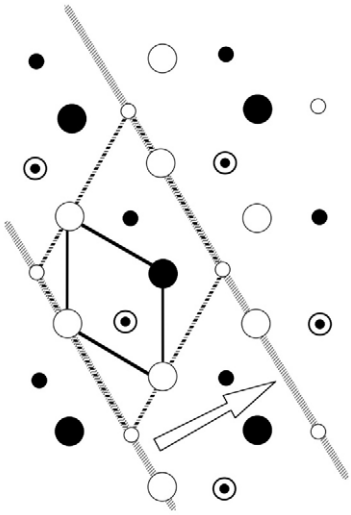

Figure 2. Spin-ordering model in the W layer [11]. The white circle is Fe^{2+} with an up-spin. The black circle is Fe^{3+} with a down-spin. The double circle is the up-spin Fe^{3+}. The spin and charge interaction is considered in the model. The charge stripe runs with the wavevector (1/3 1/3), as indicated with the white arrow.

the other 1/3 were in the opposite direction. This spin structure is considered to be a common feature in the RFe_2O_4 system.

The model for the spin arrangement in the W layer in a magnetic-ordered state was proposed as illustrated in figure 2 [11]. This model is consistent with the saturated magnetization and Mössbauer observation. In addition, the general tendency of the superexchange interaction in which antiferromagnetic coupling between Fe^{3+} and Fe^{3+} is stronger than that between Fe^{2+}–Fe^{3+} and Fe^{2+}–Fe^{2+} was regarded in the model. This consideration suggests a close relationship between the magnetic and electric structures in RFe_2O_4.

3. Dielectric response of RFe_2O_4

The dielectric response of this system provides information on the fluctuation process of the electronic structure. A large low-frequency dielectric dispersion was observed in $ErFe_2O_4$ [12–14], YFe_2O_4 [15] and $LuFe_2O_4$ [16, 17]. The response is explained by a model of the ordering of Fe^{2+} and Fe^{3+} [9]. Figure 3 shows the temperature dependence of the real and imaginary parts ε' and ε'' of the dielectric constant of the poly-crystal $LuFe_2O_4$. At low temperatures, ε' is of the order of 10. With increasing temperature, it shows an increase of about 1000 between 150 and 300 K. This shoulder shifts to higher temperatures with increasing frequency. The value of ε' reaches 3000 for higher temperatures. Correspondingly, ε'' shows a peak between 150 and 250 K. With further increasing temperature, ε' at lower frequencies reaches a small peak at around 340 K, which was confirmed as the transition temperature of the three-dimensional charge ordering, as described later. The dielectric dispersion at around 340 K is interpreted as the gradual development of the charge order coherence along the *c* axis with the variation of the dimensional change of the charge ordering from three-dimensional to

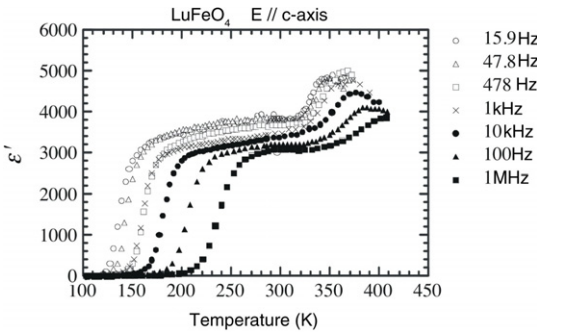

Figure 3. Temperature variation of the low-frequency dielectric constant for $LuFe_2O_4$. The dispersion below 300 K is considered as the domain boundary motion with electron exchange between Fe^{2+} and Fe^{3+}. Above 340 K, the dimensionality of the charge ordering changes from three-dimensional to two-dimensional, where the dielectric constant peak shows another dispersion.

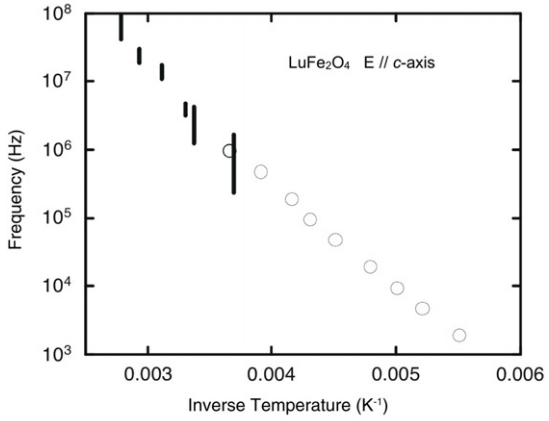

Figure 4. The peak temperature of ε'' was plotted according to the function of the frequency with a white circle. Vertical lines are the electron fluctuation frequency measured from Mössbauer spectroscopy [18]. The data demonstrates that the elementary process of the dielectric dispersion is the electron fluctuation of the iron ions.

two-dimensional above this temperature. Such dielectric dispersion was first reported in the $ErFe_2O_4$ system.

The characteristics of the dispersion were analyzed with a Cole–Cole plot indicating the superposition of a Debye-type dispersion with the narrow distribution of the relaxation time. The temperature variation of the characteristic time of the dispersion estimated from the peak of ε'' is described by an Arrhenius relation:

$$f = f_0 \exp(-Q/kT) \tag{1}$$

where f is the characteristic frequency of the dielectric response, kT is the thermal energy, f_0 is a pre-factor and Q is the activation energy. For the observation along the c axis in single-crystal $LuFe_2O_4$, f_0 and Q are 1.1×10^8 Hz and $Q = 0.25$ eV, respectively.

The relation shows that the characteristic frequency of the dispersion increases with increasing temperature. As shown by the thick vertical line in figure 4, the extrapolation of the relation coincides with the iron valence fluctuating frequency measured with Mössbauer spectroscopy [18].

In order to explain the mechanism of the dielectric dispersion, the ordering model of Fe^{2+} and Fe^{3+} was reconsidered. In the model of figure 2, the weight center of Fe^{2+} and Fe^{3+} does not coincide, i.e. the polar ordering of iron valences indicating the presence of the electric polarization in the W-layer superlattice cell. Comparing the average valence of iron of 2.5+, Fe^{2+} and Fe^{3+} behave as negative and positive charges, respectively. The electric polarization is described with the polar electron distribution on Fe^{3+}. The electron exchange process between Fe^{2+} and Fe^{3+} causes the switching of the polarization. This model explains that the electron fluctuation frequency coincides with the characteristic time of the dielectric dispersion observed in the higher-temperature region. The motion of the anti-phase boundary of the polar charge-ordered region proceeds with electron hopping from Fe^{2+} to Fe^{3+} under the application of the electric field.

The electronic ordering phenomenon as modeled in figure 2 is also explained from the frustrated interaction of Fe^{2+} and Fe^{3+} in a triangular lattice [19]. Fourier analysis of the frustrated interaction between Fe^{2+} and Fe^{3+} in the triangular geometry led to the presence of a charge stripe having a wavenumber $(1/3\ 1/3)$ in the reciprocal space, leading to the same structure as shown in figure 2.

4. Ordering of Fe^{2+} and Fe^{3+}

The superstructure shown in the W layer is the key to understanding the electric and magnetic properties of RFe_2O_4 because the frame of the superlattice cell possesses both magnetic and electric spontaneous polarization. The presence of the superstructure had first been detected with neutron diffraction as a magnetic cell. The same supercell had also been detected with electron and non-resonant x-ray diffraction, which indicated the presence of lattice distortion emerging from the ordering of Fe^{2+} and Fe^{3+}. Below 340 K, the index of the superlattice spots $(n/3\ m/3\ 0.5 + l)$, where n, m and l are integers, develops. Above 340 K, the c^* component varies to the Bragg line as $(n/3\ m/3\ L)$, where L is continuous. This shows that the three-dimensional ordering smeared out above 340 K and the ordering becomes two-dimensional that has no coherence along the c axis of the superstructure. Above about 500 K, the Bragg streak vanishes, indicating the disappearance of the superstructure. The small peak of the dielectric response found at around 340 K provided a consistent explanation that the ordering of Fe^{2+} and Fe^{3+} develops below 340 K [9].

Although the superstructure seems to arise from the ordering of Fe^{2+} and Fe^{3+}, the clarification of the origin of the superstructure was necessary. Neutron and ordinal x-ray observations are sensitive to lattice distortion but not to the charge ordering.

The application of resonant x-ray scattering (RXS) experiments is suitable for the direct detection of such charge ordering [19, 20]. Thus, RXS was performed on $LuFe_2O_4$ single crystals [21]. RXS utilizes the x-ray energy dependence of the in-phase component of the anomalous x-ray scattering factor $(f'(E))$ and its chemical shift for target ions. The

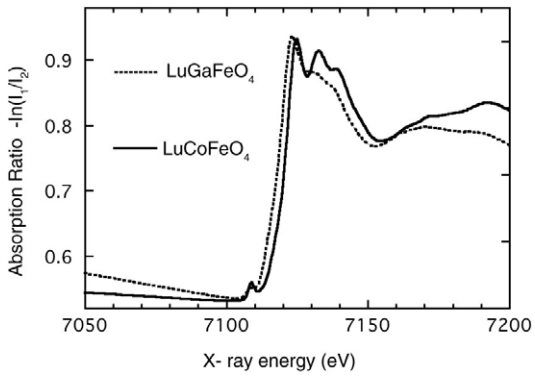

Figure 5. X-ray absorption near-edge structure (XANES) spectra near the iron K-absorption edge for $LuFeCoO_4$ and $LuFeGaO_4$, which contain Fe^{2+} and Fe^{3+}, respectively.

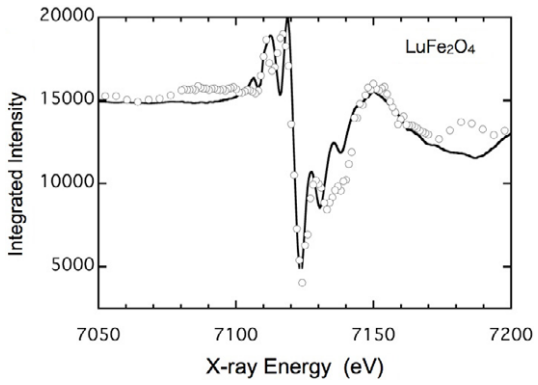

Figure 6. Circles are the x-ray energy variation for the superlattice intensity of $LuFe_2O_4$ at 15 K. The line is the difference of the $f'(E)$ between Fe^{2+} and Fe^{3+} evaluated from the XANES data [21].

$f'(E)$ is derived from the x-ray absorption near-edge structure (XANES) measurement. The XANES spectra for Fe^{2+} and Fe^{3+} were measured in powder samples of $LuFeCoO_4$, $LuFeGaO_4$ and $LuFe_2O_4$ near the iron K-absorption edge. $LuFeCoO_4$ (or $LuFeGaO_4$) is isostructural to RFe_2O_4, in which Co^{2+} (or Ga^{3+}) substitutes Fe^{2+} (or Fe^{3+}) with a solid solution. Thus, $LuFeCoO_4$ and $LuFeGaO_4$ are considered to possess a typical valence state of trivalent and divalent iron ions with a fivefold oxygen coordination of RFe_2O_4 structure.

The results of XANES spectra are shown in figure 5. As found in the figure, the absorption edge for $LuFeCoO_4$ is 3 eV higher than that of $LuFeGaO_4$. This fact shows that the excited 4p electron from the 1s state in iron of $LuFeCoO_4$ positioned in a higher potential energy caused from the higher valence state of trivalent iron. As the XANES spectra directly reflect the loss term of the anomalous atomic scattering factor $f''(E)$, we can derive the in-phase component $f'(E)$ of both Fe^{2+} and Fe^{3+} by the Kramers–Kronig (KK) transformation from the spectra. The obtained $f'(E)$ has a minimum at 7.117 and 7.120 keV for Fe^{2+} and Fe^{3+}, respectively.

When Fe^{2+} and Fe^{3+} form a superstructure, a corresponding superlattice diffraction point is contributed from the difference of the atomic scattering factors $f'(E)$ between Fe^{2+} and Fe^{3+}. Therefore, the energy variation of the diffraction intensity near the iron K-edge must indicate the presence of the differential components of $f'(E)$ between Fe^{2+} and Fe^{3+}. The RXS method is the detection of this structure factor contribution.

Figure 6 is the measured integrated intensity for $(1/3, 1/3, 6.5)$ of $LuFe_2O_4$ at 15 K, where the data was corrected for absorption. As demonstrated in the figure, the energy variation of the superlattice spot shows a characteristic enhancement, the maxima and the minima at energies of 7.116 and 7.124 keV, respectively. This is the indication of the existence of differences in the atomic scattering factor between $f'(E)$ for Fe^{2+} and Fe^{3+}, which proves the presence of the charge stripe shown in figure 2. It is noticeable that there is an independent energy component as a background to the signal in the data. This superstructure disappears at 340 K, where the low-frequency dielectric constant shows a cusp.

5. Electric polarization from the ordering of Fe^{2+} and Fe^{3+}

As reported earlier, the local electric dipole exists in this structure and gives a consistent explanation for the unique dielectric properties of these oxides. It must be emphasized that this electric polarization has a different nature from those of previously known displacement-type ferroelectrics, in which the electric dipole originates from the spontaneous polar displacement of an anion and a cation [22]. As to the origin of such a displacement, the importance of the electron transfer from an anion to a cation forming the bond of covalency was pointed out by recent first-principles calculations [23] and electron density analysis [24]. On the other hand, the polarization in RFe_2O_4 is considered as the density modulation of electrons on an average cation, $Fe^{2.5+}$ not having an associated anion. Furthermore, the charge modulation is explained by the correlated nature of electrons, the charge frustration in this case. This is a crucial difference between RFe_2O_4 and ordinary ferroelectrics of the displacement type. The switching process of the electric polarization is also a unique feature that is realized by the electron exchange among the polar ordering of Fe^{2+} and Fe^{3+}. The motion of possible ferroelectric domain boundaries proceeds as a process involving the collective motion of highly correlated electrons. This is a new aspect of the electronic behavior of the transition metal oxides.

It is commonly recognized that the ferroelectrics are defined by the polarization switching in accordance with the switching of the external electric field. Usually, the switching process is confirmed from the electric field dependence of the polarization measurement, the so-called P–E loop observation. In the case of RFe_2O_4, such typical P–E loop characteristics have rarely been reported [25]. Within our experiment, the pyroelectric measurement is an easier method to detect such polarization switching according to the electric field. Although the total dielectric properties on RFe_2O_4 have not been clarified, it is considered that the residual electronic conductivity, which inevitably arises from the 'non-charge-ordering region,' may prevent the clear observation of such P–E loop observations.

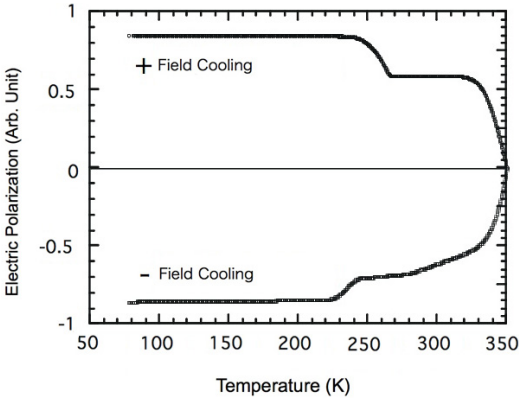

Figure 7. Temperature variation of the electric polarization estimated from the integral of the pyroelectric current measurement for the $LuFe_2O_4$ single crystal along the *c* axis [21].

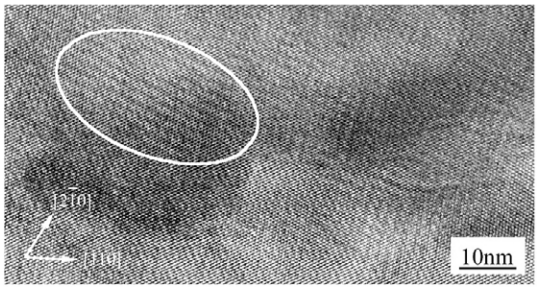

Figure 8. Charge-ordered region (circled area) observed with a transmission electron microscope for YFe_2O_4. The charge stripe with a wavenumber (1/3 1/3) is in the circle, but the wave coherence vanishes outside the circle, which demonstrates that the coherence of the charge-ordering region is about a 10 nm scale.

Previous results of the pyroelectric current observation are shown in figure 7 [17]. The data was taken from the integral of the temperature variation of the pyroelectric current in a heating process after cooling with an external electric field. The temperature variation of the current shows a characteristic peak at the magnetic transition temperature and 340 K. The latter is a three-dimensional charge-ordering temperature, and the low-frequency dielectric constant shows a small cusp. Accordingly, the electric polarization obtained from the current integral develops at this temperature. These results demonstrate the ferroelectric property of this material.

It is a noticeable coincidence that the unit cell of electric polarization, the polar distribution of Fe^{2+} and Fe^{3+}, is also the unit cell of the ferrimagnetic polarization. Then, some kind of coupling between the magnetization and electric polarization is expected. As shown in figure 7, the temperature variation of the electric polarization shows an anomaly at the magnetic transition temperature. In our preliminary observation, a slight change of the coherent length of the charge ordering at this temperature was found [26]. This is an indication of the development of spin exchange networks affected by the coherence of the charge ordering. As demonstrated in the spin-ordering model, the charge arrangement of iron ions directly couples to the spin interaction through the superexchange mechanism. Such a phenomenon is new for magnetoelectric interaction phenomena.

The ordinary magnetoelectric (ME) signal of RFe_2O_4 has been reported on poly-crystal $ErFe_2O_4$ [27]. The ME measurement was conducted with an AC electric response driven by the AC magnetic field under a DC-biased magnetic field. The sign of the signal showed a change in accordance with the cooling electric or magnetic field sign. The result was an indication of the polar property of $ErFe_2O_4$. It was also found that the AC–ME response showed a maximum when the frequency of the AC field coincided with the polarization fluctuation frequency. Recently, it was reported that $LuFe_2O_4$ shows coupling between the dielectric response and the magnetic field even at room temperature [28]. The presence of a possible residual magnetic moment at room temperature may cause such coupling [25]. The presence of such ME coupling at room temperature will be examined in the near future.

It is noticeable that the domain size of the charge-and spin-ordering region is extremely small for $LuFe_2O_4$. This was determined by electron transmission or synchrotron diffraction experiments. In figure 8, a dark-field real image of the charge-ordering region taken by a transmission electron microscope is shown. The image was taken for YFe_2O_4 having the superlattice diffraction of (1/3 1/3 1/2). In the figure, the white circle is the coherent area of the charge-ordered domain of about 10 nm [29, 30]. This is a consistent result from the x-ray diffraction experiments, in which the coherence length was estimated to be about 10 nm from the full width of the half-maximum of the peak profile within the *a*–*b* plane. In usual ferroelectrics, the long-range interaction of the lattice distortion affects the polarization domain size. The small polarization indicates that the Coulombic interaction between electronic charges dominates the total energy for the domain sizes and decoupling from the long-range interaction of the lattice distortion.

As described above, the charge model in the W layer gave a consistent explanation for the dielectric and magnetic response of RFe_2O_4. Recently, research on understanding the ground state of this material has included a wider viewpoint including the degrees of freedom of the spin, charge and orbital. The total interacted behavior of the spins, charges and orbitals of iron ions in the W layer studied using Monte Carlo calculations revealed the various magnetic and dielectric properties of this material. They revealed the orbital fluctuation by the frustrated interaction among Fe^{2+}s [31]. Furthermore, the three-dimensional spin-ordering model was proposed from the precise neutron diffraction experiment [32]. In contrast, the three-dimensional charge-ordering model in $LuFe_2O_4$, which might be the combination of six W-layer models, remains an open question.

To completely clarify the magnetism, ferroelectricity and electronic conduction properties of this material is a fascinating task in order to obtain a novel ferroelectrics application. From such interests now, the precise voltage–current characteristics of this material are currently being studied with the development of a precise sample preparation technique. The potential application of this kind of magnetoelectric interacting material might affect a large area of

technology. For example, the fast switching of the polarization realized by electronic motion without an ionic one may realize ultra-high-speed ferroelectrics. Furthermore, the electronic properties may have cross-correlation with the magnetic field, which may yield a new potential ferroelectrics application coupled with or controlled by the degrees of freedom of d-electrons, i.e. spins, charges and orbitals.

Acknowledgment

This work was partially supported by a grant from the Japanese Ministry of Education, Science, Sports, and Culture, Grant-in-Aid for Scientific Research B.

References

[1] Schmid H 1994 *Ferroelectrics* **162** 317
[2] Fiebig M 2005 *J. Phys. D: Appl. Phys.* **38** R123
[3] Tokura Y 2007 *J. Magn. Magn. Mater.* **310** 1145
[4] Kimizuka N, Muromachi E and Siratori K 1990 *Handbook on the Physics and Chemistry of Rare Earths* vol 13, ed K A Gschneidner Jr and L Eyring (Amsterdam: Elsevier) p 283
[5] Iida J, Tanaka M, Nakagawa Y, Funahashi S, Kimizuka N and Takekawa S 1993 *J. Phys. Soc. Japan* **62** 1723
[6] Akimitsu J, Inada Y, Siratori K, Shindo I and Kimizuka N 1979 *Solid State Commun.* **32** 1065
[7] Funahashi S, Akimitsu J, Siratori K, Kimizuka N, Tanaka M and Fujishita H 1984 *J. Phys. Soc. Japan* **53** 2688
[8] Katano S, Kito H, Akimitsu J, Siratori K, Funahashi S and Child H R 1995 *Physica* B **213/214** 215
[9] Yamada Y, Nohdo S and Ikeda N 1997 *J. Phys. Soc. Japan* **66** 3733
[10] Tanaka M, Iwasaki H, Siratori K and Shindo I 1989 *J. Phys. Soc. Japan* **58** 1433
[11] Siratori K, Funahashi S, Iida J and Tanaka M 1992 *Ferrites, Proc. 6th Int. Conf. on Ferrites* (Tokyo: The Japan Society of Powder and Powder Metallurgy) p 703
[12] Ikeda N, Kito H, Akimitsu J, Kohn K and Siratori K 1994 *J. Phys. Soc. Japan* **63** 4556
[13] Ikeda N, Kohn K, Kito H, Akimitsu J and Siratori K 1995 *J. Phys. Soc. Japan* **64** 1371
[14] Ikeda N, Odaka K, Takahashi E, Kohn K and Siratori K 1997 *Ferroelectrics* **190** 191
[15] Ikeda N, Mori R, Kohn K, Mizumaki M and Akao T 2002 *Ferroelectrics* **272** 175
[16] Takahashi E, Kohn K and Ikeda N 1998 *J. Korean Phys. Soc.* **32** S44
[17] Ikeda N, Kohn K, Myouga N, Takahashi E, Kitôh H and Takekawa S 2000 *J. Phys. Soc. Japan* **69** 1526
[18] Tanaka M, Siratori K and Kimizuka N 1984 *J. Phys. Soc. Japan* **53** 760
[19] Sasaki S 1995 *Rev. Sci. Instrum.* **66** 1573
[20] Murakami Y, Kawada H, Kawata H, Tanaka M, Arima T, Moritomo Y and Tokura Y 1998 *Phys. Rev. Lett.* **80** 1932
[21] Ikeda N *et al* 2005 *Nature* **436** 1136
[22] Kittel C 1995 *Introduction to Solid State Physics* (New York: Wiley)
[23] Cohen R E 1992 *Nature* **358** 136
Sághi-Szabó G, Cohen R E and Krakauer H 1998 *Phys. Rev. Lett.* **80** 4321
[24] Kuroiwa Y, Aoyagi S, Sawada A, Harada J, Nishibori E, Takata M and Sakata M 2001 *Phys. Rev. Lett.* **87** 217601
[25] Park J Y, Park J H, Jeong Y K and Lang H M 2007 *Appl. Phys. Lett.* **91** 152903
[26] Kakurai K 2008 private communication
[27] Ikeda N, Saito K, Kohn K, Kito H, Akimitsu J and Siratori K 1994 *Ferroelectrics* **161** 111
[28] Subramanian M A, He T, Chen J Z, Chen J, Rogado N S, Calvarese T G and Sleight A W 2006 *Adv. Mater.* **18** 1737
[29] Horibe Y, Kishimoto K, Mori S and Ikeda N 2005 *J. Electron Microsc.* **54** i87
[30] Murakami Y, Abe N, Arima T and Shindo T 2007 *Phys. Rev.* B **76** 024109
[31] Nagano A, Naka M, Nasu J and Ishihara S 2007 *Phys. Rev. Lett.* **99** 217202
[32] Christianson A D, Lumsden A M, Angst Yamani Z, Tian W, Jin R, Payzant E A, Nagler S E, Sales B C and Mandrus D 2008 *Phys. Rev. Lett.* **100** 107601